Astron. Astrophys. 94, 116–120 (1981)

ASTRONOMY AND ASTROPHYSICS

Search for γ-radiation from Extragalactic Objects Using a Likelihood Method

A. M. T. Pollock[5,*], G. F. Bignami[2], W. Hermsen[1], G. Kanbach[4], G. G. Lichti[6,**], J. L. Masnou[5], B. N. Swanenburg[1], and R. D. Wills[6]

[1] Cosmic Ray Working Group, Huygens Laboratorium, Leiden, The Netherlands
[2] Istituto di Fisica Cosmica del CNR, Milan, Italy
[3] Istituto di Fisica, Università di Palermo, Palermo, Italy
[4] Max-Planck-Institut für Extraterrestrische Physik, D-8046 Garching bei München, Federal Republic of Germany
[5] Division de la Physique, Section d'Astrophysique, Centre d'Études Nucléaires de Saclay, B.P. 2, F-91190 Gif-sur-Yvette, France
[6] Space Science Department of ESA, ESTEC, Noordwijk, The Netherlands

Received March 27, accepted June 24, 1980

Summary. A search through COS-B data for γ-radiation from a number of extragalactic objects reveals no strong evidence for any positive identification except, as already reported, for the region around the quasar 3C273. Upper limits to the photon fluxes from active extragalactic objects are evaluated using a likelihood method. They reinforce the conclusion reached by Bignami et al. (1979) from the SAS-2 data that the flux upper limits lie substantially below the extrapolation of spectra measured at X-ray energies. The proposed identifications of 2CG135+01 are also discussed.

Key words: active galaxies – γ-ray sources – COS-B – γ-ray astronomy

I. Introduction

The identification of quasars, Seyfert and other active galaxies as general classes of X-ray sources has been established through the work of the groups attached to the Ariel V, *Uhuru*, and SAS-3 satellites, and more recently, the HEAO series. Measurements of these objects are now available variously from radio through to X-ray frequencies and it is therefore an opportune moment to publish the high-energy γ-ray observations that are available. The SAS-2 results, which cover the energy range above 35 MeV, have been published recently (Bignami et al., 1979). The present paper gives the results of a search in the COS-B data for evidence of γ-ray emission above 50 MeV from a number of extragalactic objects. The larger part of the COS-B programme has been dedicated to a survey of the galactic plane (Mayer-Hasselwander et al., 1980) but high-latitude measurements are also available. A search for γ-ray sources using a cross-correlation method led to the discovery of excess γ-ray emission from the sky in the region of 3C273 (Swanenburg et al., 1978; Bignami et al., 1980). Consideration of possible emission from specific objects allows the use of a different method based on the likelihood function. This method has particular advantages in the estimation of source parameters.

II. Method of Analysis

The approach to statistical inference employed in this paper has been particularly encouraged by Edwards (1972). Its central idea is summed up in the likelihood axiom:

"Within the framework of a statistical model, all the information which the data provide concerning the relative merits of two hypotheses is contained in the likelihood ratio of those hypotheses on the data, and the likelihood ratio is to be interpreted as the degree to which the data support the one hypothesis against the other."

The likelihood ratio allows a choice between specific hypothesis: in particular between different statistical models or different values in a particular model. In the present context the different hypotheses are characterised by different values of X, the fraction of the observed photons attributable to a point source. To be specific, with attention confined to parts of the sky in which the background is uniform, the probability of observing a photon in the solid angle element $d\Omega$, centred at coordinates (α, δ) in the region Ω can be written as

$$p(\alpha, \delta, A, B)d\Omega = (AS(\theta) + B)d\Omega, \quad (1)$$

where $\int_\Omega p d\Omega = 1$.

The function $S(\theta)$ describes the response of the detector to a point source and depends only on θ, the angle between the source and the reconstructed photon trajectory. It is known from calibration measurements which have been confirmed through observation of the pulsed radiation of the Vela pulsar (Scarsi et al., 1977; Hermsen, 1980). The data have been divided into the energy ranges 50–150 and 150–5000 MeV, for which

$$(\theta) = \frac{\int \theta S(\theta) d\Omega}{\int S(\theta) d\Omega} \quad (2)$$

is about 5° and 3° respectively. A compromise must be sought between the ability to collect all the photons from a source and possible confusion from large-scale gradients in the data or from other objects. Therefore all the photons observed within angles, θ_{max}, of 7.5° and 5° at low and high energy respectively have been used. This involves renormalisation by factors of 1.25 and 1.10 to convert to the entire flux from the source. The constants A and B

Send offprint request to: J. L. Masnou

* Present address: Department of Space Research, University of Birmingham, UK

** Present address: Max-Planck-Institute für Extraterrestrische Physik, D-8046 Garching bei München, Federal Republic of Germany

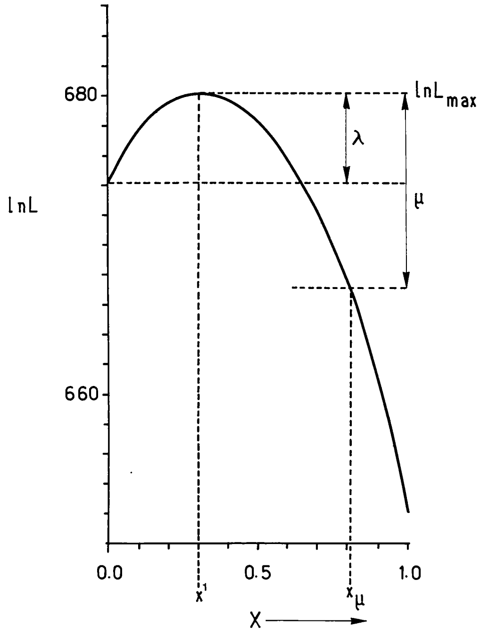

Fig. 1. An idealised likelihood curve showing the value of X best supported by the data (x^1) and the upper limit (x_μ) corresponding to a ratio of e^μ between the likelihood of $X=x_1$ and $X=x_\mu$. The parameter λ is defined in the text

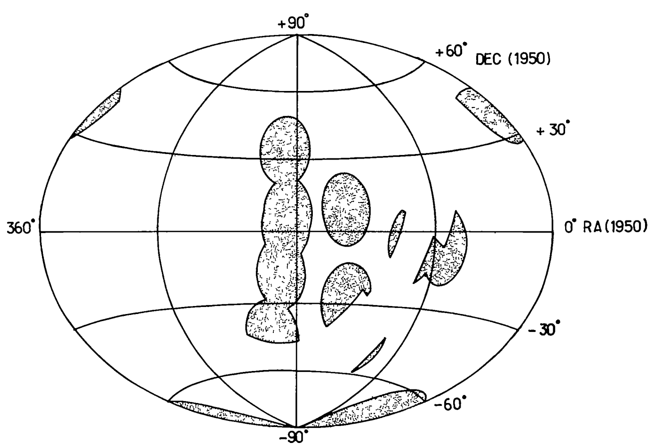

Fig. 2. Regions of the sky used in the present search (shaded). The regions at low galactic latitude were excluded because of the non-uniform background

in Eq. (1) give the relative contribution of source and background and are related through the normalisation of p. For the N photons observed within θ_{max} the likelihood then reduces to a function of the single parameter, X, the fraction of photons from the source at $\theta=0$,

$$L(X)=\prod_{i=1}^{N}\left(\frac{XS(\theta_i)}{I}+\frac{1-X}{2\pi(1-\cos\theta_{max})}\right)$$

with

$$I=2\pi\int_0^{\theta_{max}} S(\theta)\sin\theta\, d\theta$$

and $X=AI$.

Table 1. COS-B observations used in the search

Observation no.	Epoch from	Epoch to	Pointing Direction (1950.0) R.A.	dec.
3	1975–10–20	1975–11–28	8h 31m 8h 57m	−45° −40°
6	1976–01–23	1976–02–23	13h 16m	−44°
10	05–24	06–24	12h 21m	+ 7°
12	07–24	08–21	8h 56m	−41°
15	11–02	12–10	1h 10m	−74°
19	03–07	04–14	7h 1m	− 6°
20	04–14	05–02	9h 40m	−28°
23	07–15	08–18	12h 40m	−18°
27	12–07	1978–01–13	12h 31m	+34°
31	1978–05–03	06–09	9h 51m	+ 9°
32	06–09	07–17	12h 26m	+ 2°
34	08–23	09–29	5h 33m	− 5°
37	12–11	1979–01–17	0h 24m	+42°

For convenience the natural logarithm of the likelihood will be used:

$$\ln L(X)=\sum_{i=1}^{N}\ln\left(\frac{XS(\theta_i)}{I}+\frac{1-X}{2\pi(1-\cos\theta_{max})}\right).$$

The parameter $\ln L(X)$ is a relative measure of how well the data support the hypothesis $X=x$; if $\ln L(x_1)>\ln L(x_2)$ then x_1 is a better value than x_2. All the information about X is contained in the curve $\ln L(X)$ against X. In general this curve shows a maximum corresponding to the value of X best supported by the data (see Fig. 1). Upper limits on the intensities of candidate sources may be derived by determining the value of X at which $\ln L$ falls to some value $\ln L_{max}-\mu$. A value of $\mu=2$ corresponds to a ratio of $e^\mu=7.4$ between the likelihood of the best supported value of X and the upper limit. In a classical treatment of Gaussian statistics this would correspond to a confidence level of 2σ. In cases where the parameter

$$\lambda=\ln L_{max}-\ln L(X=0)>\mu$$

it is possible to define also an equivalent lower limit. However it should be remembered that it is usual practice to demand stronger evidence, of which λ provides a continuous scale, before a measurement of a positive signal from a source is claimed.

III. Application to the COS-B Data

Away from the galactic disk, the flux detected by COS-B, consists mainly of a high particle background, of the residual galactic emission and of the isotropic flux (Fichtel et al., 1978). We have restricted our study to those regions of the sky above a longitude dependent latitude limit where inspection reveals that the background is adequately described as uniform over the field used for the search. The list of the observations available under these conditions is given in Table 1. The sky coverage thus achieved is shown in Fig. 2. The objects studied were those within 15° of a COS-B pointing direction which appear in the following lists:

1. Seyfert galaxies (Weedman, 1977) with several additions of galaxies identified through their X-ray emission;

2. quasars (Burbidge et al., 1977) arbitrarily selected with visual magnitude $m_v < 16.5$;

3. BL Lac objects (Stein et al., 1976);

4. assorted active galaxies, including N galaxies and other emission line galaxies that are known as X-ray sources (Marshall et al., 1978);

5. some galaxies in the local group (Kraan-Korteweg and Tammann, 1979).

The results in the two energy intervals are shown in Tables 2a and 2b where each object is accompanied by

1. the position;
2. cz, in km s^{-1};
3. N, the number of photons in the $\theta_{\max}$ degree circle;
4. $\lambda = \ln L_{\max} - \ln L(X=0)$;
5. a tabulation of the $\ln L$ curve in the form of the values $n_j^{\pm}$, the numbers of photons from the object for which $\ln L$ is a maximum and for which it has fallen 1, 2, and 3 below the maximum;
6. the photon flux in cm^{-2} s^{-1} as an upper limit corresponding to n_2^+;
7. the COS-B observation periods from which the data were obtained.

It is seen that the highest value of $\lambda(5.9)$ is associated with the quasar 1226+023 (3 C 273) above 150 MeV. This corresponds to a likelihood ratio of 376 whereas the next highest value (3.6) corresponds to a ratio of only 38. There is thus strong evidence for an excess in the region of 3 C 273.

In order to investigate how well this excess is associated with the quasar, a similar procedure to that used above in connection with X can be used jointly for X, α_0, δ_0 where α_0, δ_0 are the coordinates of the γ-ray source. Thus

$$\ln L(X, \alpha_0, \delta_0) = \sum_{i=1}^{N} \ln\left(\frac{X S(\theta_i')}{I'} + \frac{(1-X)}{2\pi(1-\cos\theta_{\max})}\right),$$

where

$$I' = \int_0^{2\pi} d\phi \int_0^{\theta_{\max}} d\theta \sin\theta\, S(\theta'),$$

and θ' is the angle between the supposed position (α_0, δ_0) of the source (θ_0, ϕ_0) in the coordinate system centred on the object and the photon direction α, $\delta(\theta, \phi)$.

Again, all the information about X, α_0, δ_0, any one of which cannot be considered independently of the other two, is contained in the surface $\ln L(x, \alpha_0, \delta_0)$ in three-dimensional parameter space. However, in order to give an indication of the values of α_0 and δ_0 which are supported by the data, Fig. 3 shows contours of $\ln L_{\max}(\alpha_0, \delta_0)$ which is the logarithm of the likelihood at α_0, δ_0 for the value of X which maximises it. $X_{\max}$ is not the same at every point. The regions traced out in this way give a good idea of the weight to be attached to each possible position because the likelihood at all other values of X other than those implicit in the diagram is smaller. The contours are at values of $\ln L = 1$, 2, and 3 below the maximum with respect to X, α_0, and δ_0 jointly.

This figure is strong evidence for the association of the excess with 3 C 273, supporting the identification of CG 291+65 (Swanenburg et al., 1978; Bignami et al., 1980). A secondary conclusion from the figure is that the values of λ associated in the tables with Mkn 50 are mainly due to counts from 3 C 273 which is only 1°.6 away. In other words, it is probable that a single excess is responsible for the results of both objects. Use of the likelihood ratio for the photons above 150 MeV (where the resolution is better) in the circle centred on the point midway between the two objects, allows a direct comparison between the 3 hypotheses:

Table 2a. 50 – 150 MeV

	RA	DEC	CZ	N	λ	n_3^-	n_2^-	n_1^-	n_0	n_1^+	n_2^+	n_3^+	FLUX LIM.	OBSERVATIONS
SEYFERT TYPE 1 GALAXIES														
ZWICKY1	9.9	40.1	18280	101	0.2				8.4	31.4	41.4	49.3	2.1E-06	37
MKN352	14.3	31.6	4500	63	3.3	1.4	6.5	13.7	32.6	51.8	59.6	65.5	3.9E-06	37
AKN42	20.5	31.9	10800	56	0.0				0.1	15.5	22.5	28.0	1.7E-06	37
MKN358	20.9	31.3	13750	50	0.4				8.0	23.4	30.1	35.3	2.4E-06	37
AKN120	78.4	-0.2	9900	123	0.0				0.0	12.7	21.8	29.4	1.4E-06	34
ZWICKY2	145.6	1.3	15200	119	0.0				0.0	22.6	33.9	42.9	2.6E-06	31
3C227	146.3	7.7	25600	134	2.7		5.3	15.5	41.6	69.3	81.0	89.9	5.4E-06	31
AKN223	148.7	7.4	6600	137	0.1				8.1	36.2	48.5	58.1	3.2E-06	31
NGC4051	180.1	44.8	700	48	0.0				3.5	21.9	29.8	35.9	2.3E-06	27
NGC4151	182.0	39.7	990	69	1.0			0.3	19.3	40.7	49.6	56.4	2.8E-06	27
MKN50	185.2	3.0	6910	238	2.4		4.0	18.3	55.2	94.3	110.9	123.8	2.7E-06	10,32
X COMAE	194.5	28.7	27600	93	0.0				0.0	11.4	19.7	26.7	1.1E-06	27
MKN64	196.2	34.7	55200	85	1.3			2.6	23.7	47.0	56.9	64.5	3.1E-06	27
IC4329A	206.6	-30.0	4140	126	0.0				2.9	26.7	37.3	45.6	3.3E-06	6
ESO113-IG45	20.5	-59.1	13800	128	0.0				0.0	12.1	20.7	27.8	1.5E-06	15
MKN348	11.5	32.6	4200	67	3.6	3.2	9.5	18.1	39.2	61.7	70.3	76.7	4.2E-06	37
MKN1	18.3	32.8	4800	60	1.2			2.0	21.5	43.2	52.0	58.5	3.5E-06	37
NGC3227	155.2	20.1	1000	66	0.7				14.1	33.4	41.6	47.8	4.6E-06	31
SEYFERT TYPE 2 GALAXIES														
NGC4507	188.2	-39.6	3310	159	0.0				1.4	27.6	39.7	49.1	2.3E-06	6
MKN268	204.7	30.6	12300	51	0.2				6.8	23.4	30.8	36.6	2.7E-06	27
QUASARS														
0134+329	23.7	32.9	110000	38	0.0				0.4	15.6	22.2	27.3	1.9E-06	37
0454+039	73.5	3.9	404000	85	0.0				0.0	15.7	24.0	30.6	2.3E-06	34
0736+017	114.2	1.7	57300	86	1.0				23.0	47.8	58.5	66.6	3.8E-06	19
1001+054	150.4	5.5	48300	128	0.5				18.0	47.5	59.9	69.4	4.2E-06	31
1004+130	151.2	13.1	71900	104	0.0				0.0	9.9	17.5	23.9	1.3E-06	31
1128+315	172.1	31.5	86600	55	0.4				9.5	27.2	35.0	41.1	2.8E-06	27
1146-037	176.6	-3.8	102000	171	1.5			5.1	32.2	61.7	74.4	84.2	2.7E-06	10,32
1156+295	179.2	29.5	219000	81	0.0				1.7	23.4	32.9	40.3	1.9E-06	27
1202+281	180.5	28.2	495000	80	0.1				4.5	25.9	35.2	42.6	2.0E-06	27
1208+322	182.0	32.2	116000	90	0.9				20.3	44.1	54.5	62.6	2.8E-06	27
1215+113	184.0	11.4	419000	198	0.0				0.0	30.1	44.5	55.8	1.2E-06	10,32
1223+252	185.8	25.2	80300	82	0.0				0.1	18.1	26.3	32.8	1.5E-06	27
1225+310	186.3	31.0	660000	102	0.8				21.2	46.7	57.6	66.0	2.8E-06	27
1226+023	186.6	2.3	47400	242	2.2		2.6	16.6	53.4	92.1	108.7	121.7	2.6E-06	10,32
1229+204	187.5	20.4	19200	122	0.0				0.0	17.0	27.0	35.1	1.1E-06	10,27
1302-102	195.7	-10.3	85700	78	0.0				2.5	20.6	28.8	35.2	1.6E-06	23
1317+277	199.3	27.7	306000	71	0.2				8.3	27.7	36.3	42.9	2.4E-06	27
1318+291	199.7	29.1	511000	66	0.9				17.7	39.1	48.1	55.0	3.2E-06	27
1321+294	200.3	29.5	288000	69	0.3				10.4	30.9	39.8	46.5	2.7E-06	27
1355-416	209.0	-41.6	93800	180	0.5				21.3	54.5	69.0	80.2	3.8E-06	6
BL LAC OBJECTS														
0957+226	149.4	22.6		73	0.0				0.0	11.2	18.7	24.9	2.1E-06	31
1147+245	176.9	24.6		53	1.0			0.0	17.5	36.4	44.2	50.0	3.4E-06	27
1215+303	183.9	30.3		96	0.9				19.5	43.3	53.4	61.3	2.7E-06	27
1219+285	184.9	28.5		93	0.2				10.6	34.2	44.5	52.4	2.3E-06	27
1225+206	186.4	20.6		122	0.0				0.0	11.4	20.4	28.0	8.1E-07	10,27
1307+121	196.9	12.2		186	0.2				12.1	45.3	59.6	70.8	2.3E-06	10,32
ASSORTED ACTIVE GALAXIES														
NGC2110	87.4	-7.5	2100	138	0.0				4.4	32.3	44.7	54.4	2.8E-06	34
NGC2992	145.8	-14.1	2200	30	0.0				0.0	8.9	14.0	18.1	2.1E-06	20
MCG5-23-16	145.9	-30.4	2450	253	0.9				31.7	67.6	83.1	95.2	2.4E-06	3,12,20
M87	187.1	12.7	1210	176	1.0			0.4	27.7	57.7	70.6	80.7	2.0E-06	10,32
CEN A	200.6	-42.8	250	227	0.0				5.6	37.6	52.1	63.5	2.5E-06	6
LOCAL GROUP GALAXIES														
NGC147	7.6	48.2	37	110	0.2				8.9	32.5	42.9	51.0	2.5E-06	37
ANDIII	8.2	36.2	37	97	0.0				0.0	9.9	17.7	24.4	9.5E-07	37
NGC185	9.1	48.1	37	105	0.2				9.4	33.1	43.7	52.0	2.5E-06	37
NGC205	9.4	41.4	37	95	1.2			1.6	22.8	46.4	56.4	64.1	2.8E-06	37
M32	10.0	40.6	37	98	0.5				15.3	38.5	48.5	56.3	2.4E-06	37
M31	10.0	41.0	37	96	0.8				19.3	42.7	52.7	60.4	2.6E-06	37
ANDI	10.8	37.7	37	95	0.0				0.8	26.1	37.5	46.4	1.9E-06	37
SMC	12.7	-73.1	3	384	0.0				0.0	8.5	16.3	23.8	6.3E-07	15
ANDII	18.4	33.2	37	60	1.1			0.6	21.5	43.8	52.8	59.6	3.5E-06	37
M33	22.8	30.4	45	37	0.8				12.0	27.0	33.2	37.8	3.1E-06	37

Table 2b. 150 – 5000 MeV

	RA	DEC	CZ	N	λ	n_3^-	n_2^-	n_1^-	n_0	n_1^+	n_2^+	n_3^+	FLUX LIM.	OBSERVATIONS
SEYFERT TYPE 1 GALAXIES														
ZWICKY1	9.9	40.1	18280	35	0.0				0.0	3.7	6.8	9.6	1.1E-07	37
MKN352	14.3	31.6	4500	16	0.0				0.0	4.9	7.7	9.8	1.8E-07	37
AKN42	20.5	31.9	10800	24	2.8		1.6	4.5	12.6	20.8	23.9	26.0	6.7E-07	37
MKN358	20.9	31.3	13750	25	1.2			0.7	8.4	16.8	20.1	22.5	6.1E-07	37
AKN120	78.4	-0.2	9900	61	0.0				0.0	4.6	8.5	11.9	1.9E-07	34
ZWICKY2	145.6	1.3	15200	25	0.0				0.0	8.3	12.3	15.2	3.3E-07	31
3C227	146.3	7.7	25600	37	1.8			2.5	10.9	20.0	23.7	26.5	5.0E-07	31
AKN223	148.7	7.4	6600	35	0.0				0.0	9.2	14.0	17.8	2.9E-07	31
NGC4051	180.1	44.8	700	26	2.1		0.1	2.6	10.1	18.6	21.9	24.4	6.2E-07	27
NGC4151	182.0	39.7	990	28	0.0				0.0	4.8	8.0	10.7	1.6E-07	27
MKN50	185.2	3.0	6910	127	2.9		3.9	9.8	25.8	43.5	51.2	57.1	3.9E-07	10,32
X COMAE	194.5	28.7	27600	25	0.8				7.5	18.2	22.6	25.7	4.2E-07	27
MKN64	196.2	34.7	55200	21	0.3				4.5	13.7	17.3	19.9	3.2E-07	27
IC4329A	206.6	-30.0	4140	49	0.0				0.0	4.8	8.8	12.4	3.0E-07	6
ESO113-IG45	20.5	-59.1	13800	34	0.0				0.0	3.1	5.7	8.1	1.6E-07	15
MKN348	11.5	32.6	4200	20	0.0				0.6	6.6	9.5	11.8	2.0E-07	37
MKN1	18.3	32.8	4800	24	0.6				6.2	15.0	18.5	21.0	4.5E-07	37
NGC3227	155.2	20.1	1000	26	0.0				0.0	3.2	5.9	8.3	2.5E-07	31
SEYFERT TYPE 2 GALAXIES														
NGC4507	188.2	-39.6	3310	57	0.0				0.0	6.0	10.2	13.8	2.2E-07	6
MKN268	204.7	30.6	12300	13	0.7				4.5	10.7	12.9		4.3E-07	27
QUASARS														
0134+329	23.7	32.9	110000	26	0.0				0.0	6.1	9.6	12.4	3.1E-07	37
0454+039	73.5	3.9	404000	35	0.2				4.1	14.3	18.7	22.1	6.7E-07	34
0736+017	114.2	1.7	57300	30	2.1		0.2	2.7	10.2	18.8	22.3	24.9	5.4E-07	19
1001+054	150.4	5.5	48300	31	0.0				0.0	5.8	9.5	12.6	2.1E-07	31
1004+130	151.2	13.1	71900	29	0.0				0.0	3.5	6.5	9.2	1.5E-07	31
1128+315	172.1	31.5	86600	15	0.0				0.0	5.7	8.7	10.8	2.6E-07	27
1146-037	176.6	-3.8	102000	61	0.0				0.0	5.8	10.0	13.4	1.4E-07	10,32
1156+295	179.2	29.5	219000	23	0.0				0.0	4.9	8.2	10.9	1.6E-07	27
1202+281	180.5	28.2	495000	23	0.0				0.0	5.4	8.8	11.6	1.7E-07	27
1208+322	182.0	32.2	116000	26	0.0				0.0	3.1	5.7	8.1	9.6E-08	27
1215+113	184.0	11.4	419000	88	0.0				0.0	5.1	9.5	13.5	8.7E-08	10,32
1223+252	185.8	25.2	80300	22	0.5				4.3	11.7	15.0	17.5	3.0E-07	27
1225+310	186.3	31.0	660000	30	0.0				0.0	9.4	13.7	17.0	2.1E-07	27
1226+023	186.6	2.3	47400	121	5.9	10.2	15.3	22.2	40.2	59.2	67.2	73.3	5.2E-07	10,32
1229+204	187.5	20.4	19200	38	1.0			0.1	8.6	18.7	23.0	26.3	3.4E-07	10,27
1302-102	195.7	-10.3	85700	36	1.8			2.6	11.5	21.2	25.2	28.2	5.2E-07	23
1317+277	199.3	27.7	306000	13	0.5				4.8	12.1				27
1318+291	199.7	29.1	511000	18	0.0				0.0	3.6	6.3	8.5	1.5E-07	27
1321+294	200.3	29.5	288000	17	0.0				0.0	3.1	5.6	7.6	1.4E-07	27
1355-416	209.0	-41.6	93800	89	0.0				1.4	17.7	24.9	30.4	4.8E-07	6
BL LAC OBJECTS														
0957+226	149.4	22.6		26	0.0				0.0	4.0	7.1	9.7	3.1E-07	31
1147+245	176.9	24.6		16	0.0				0.0	7.6	11.5	14.3	3.3E-07	27
1215+303	183.9	30.3		26	0.5				4.6	12.4	15.9	18.6	2.6E-07	27
1219+285	184.9	28.5		26	0.7				6.6	16.0	19.1	21.7	3.2E-07	27
1225+206	186.4	20.6		36	3.6	1.2	3.6	7.0	16.4	26.1	30.1	33.0	4.5E-07	10,27
1307+121	196.9	12.2		48	2.8		2.0	5.7	16.1	27.7	32.7	36.4	4.8E-07	10,32
ASSORTED ACTIVE GALAXIES														
NGC2110	87.4	-7.5	2100	109	0.0				0.0	13.0	19.7	25.2	4.0E-07	34
NGC2992	145.8	-14.1	2200	17	0.0				0.0	2.9	5.4	7.6	3.1E-07	20
MCG5-23-16	145.9	-30.4	2450	116	1.6			4.4	21.3	39.7	47.5	53.5	4.9E-07	3,12,20
M87	187.1	12.7	1210	62	0.0				0.0	10.4	15.4	19.3	1.5E-07	10,32
CEN A	200.6	-42.8	250	91	1.6			3.5	18.0	34.0	40.9	46.3	6.2E-07	6
LOCAL GROUP GALAXIES														
NGC147	7.6	48.2	37	51	0.0				0.0	3.9	7.2	10.2	1.4E-07	37
ANDIII	8.2	36.2	37	32	0.4				4.9	14.4	18.5	21.7	3.2E-07	37
NGC185	9.1	48.1	37	44	0.0				0.0	3.9	7.3	10.2	1.4E-07	37
NGC205	9.4	41.4	37	31	0.0				0.5	8.1	11.7	14.6	1.8E-07	37
M32	10.0	40.6	37	34	0.0				0.0	4.0	7.2	9.9	1.1E-07	37
M31	10.0	41.0	37	31	0.0				0.0	5.5	9.1	11.9	1.4E-07	37
ANDI	10.8	37.7	37	31	0.1				2.7	11.9	16.0	19.2	2.6E-07	37
SMC	12.7	-73.1	3	90	0.1				4.2	19.0	25.6	30.8	3.1E-07	15
ANDII	18.4	33.2	37	25	0.7				6.1	14.5	17.9	20.4	4.3E-07	37
M33	22.8	30.4	45	22	0.2				3.1	11.3	14.9	17.5	5.3E-07	37

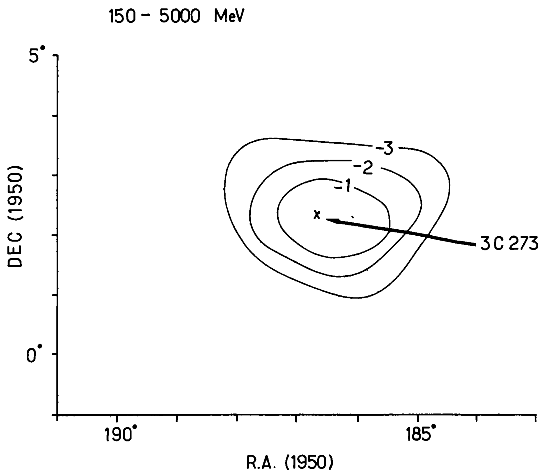

Fig. 3. Contours of constant likelihood for the location of a point source of 150 to 5000 MeV γ-rays in the region of 3 C 273. The contours are spaced at unit logarithmic intervals below the maximum value of 5.9. The actual position ($\alpha = 186.63°$, $\delta = 2.33°$) of 3 C 273 is also shown

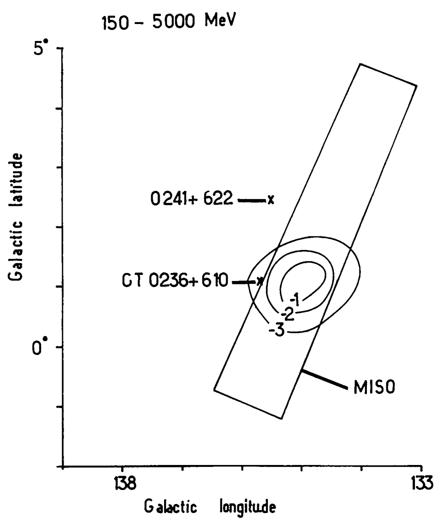

Fig. 4. Contours of constant likelihood for the location of a point source of 150 to 5000 MeV γ-rays in the region of the quasar 0241 + 622 and the radio-source GT 0236 + 610. Also shown is the MISO error box (Della Ventura et al., 1979)

---

1. there is one source at the position of 3 C 273;
2. there is one source at the position of Mkn 50;
3. there is a source at both positions.

The following results emerge:

3 C 273: $\lambda = 5.7$ at $X = 0.28$
Mkn 50: $\lambda = 3.9$ at $X = 0.22$
Both: $\lambda = 6.3$ at X (3 C 273) $= 0.22$
X (Mkn 50) $= 0.10$.

These values of λ are immediately comparable because $\ln L(X=0)$ is the same for each being the logarithm of the likelihood for a uniform distribution of photons. Clearly the data are better described by a point source at the position of 3 C 273 rather than Mkn 50. Assuming the quasar to be emitting, a small improvement in λ can be achieved through the addition of a contribution from the Seyfert galaxy. However, this procedure could be continued almost indefinitely by adding point sources at every position at which the photon density is higher than average, finally resulting in a large λ from a meaningless probability model. The addition of a further source, or in general a further degree of freedom, can be justified by a sufficiently large increase in λ, say 2. Here the increase is 0.6, not enough to do so. Thus we may state that, due to the presence of an excess near Mkn 50 that is probably attributable to another source, we are not able to determine much about its γ-ray characteristics.

IV. The γ-ray Source CG 135 + 01

Although the distribution of the COS-B γ-ray sources (Hermsen et al., 1977; Wills et al., 1980) suggests that the majority of them are galactic in nature, an X-ray investigation of CG 135 + 1 led to the discovery of the low-redshift quasar 0241 + 622 (Apparao et al., 1978). In addition the highly variable radio source GT 0236 + 610 (Gregory and Taylor, 1978; Gregory et al., 1979) has also been proposed as an identification of CG 135 + 1. The two candidates are separated by 1.°3. The relative merits of the two propositions can be examined as before with the likelihood. Some complication is introduced by the proximity of the galactic plane, the emission of which must be included in the probability model. There are three components to the observed radiation: the source, the plane and the isotropic background, which includes an instrumental contribution. The measurements presented by Mayer-Hasselwander et al. (1980) show that the ratio of the maximum plane intensity to the isotropic background is approximately 2.2 in this region. Several forms of the galactic emission have been tried, all Gaussians, of half width $w = 3°$, 5° and 7° centred on $b = 0°$ and $b = 1.4°$ to take account of the so-called hat-brim effect (Mayer-Hasselwander et al., 1980). The highest likelihood comes from $b = 0°$, $w = 5°$ when the two objects compare thus:

0241 + 622: $\lambda = 1.8$ at $X = 0.1$
GT0236 + 610: $\lambda = 6.3$ at $X = 0.2$
Both: $\lambda = 6.3$ at X (0241) $= 0.0$
X (0236) $= 0.2$

Although these results must be viewed a little circumspectly because of their dependence on a rather complicated probability model, there is strong evidence in favour of GT 0236 + 610 rather than the quasar. In fact every model tried gave $\lambda(0236) > \lambda(0241)$. Figure 4 shows the likelihood contours for the position of CG 135 + 1 along with the error box for the low energy γ-ray emission around 1 MeV in this region observed by the MISO telescope (Della Ventura et al., 1979).

V. Discussion

Although it is dangerous to compare upper limits determined in different ways and for different energy ranges, the values presented here are in some cases more restrictive than those from SAS-2. Therefore the results presented in Table 1 reinforce the conclusion of Bignami et al. (1979) concerning the spectrum of active galaxies in general: the extrapolation of X-ray spectra over three or more decades of energy would give photon fluxes substantially higher than the observed upper limits. There must be a significant steepening of the spectrum between the X-ray and the γ-ray regions. A variation of this form has been measured by Perotti et al. (1980) during an observation of NGC 4151 around 3 MeV.

Acknowledgements. GGL acknowledges the receipt of an ESA fellowship and AMTP a fellowship awarded by the Royal Society under the European Exchange Scheme. J.L. Masnou thanks the CENTRE NATIONALE DE LA RECHERCHE SCIENTIFIQUE for support.

Appendix

Statisticians are broadly divided into two factions, Bayesian and classical, each unable to support the fundamental notions of the other. In the classical approach to statistical inference, parameters are estimated with associated confidence limits from various combinations of the measurements that were made. One then appeals to a hypothetical infinite series of observations made under supposedly identical conditions to say, for example, that 90% of all confidence intervals drawn up in this way will contain the true value of the parameter under study. Whether the interval that has been drawn up from the experimental results does so or not is unknown. Critics of the classical scheme question the justification of assigning asymptotic properties to particular estimates.

All Bayesian statements about parameters are probability statements of the type $P(a<\mu<b)=\alpha$, which, in contrast to the frequency notion, is to be interpreted as a degree of belief about the parameter μ. In order to achieve this, previous knowledge about the parameter, in the form of a prior probability distribution, is combined with the information obtained from the data, the likelihood, to yield a posterior probability distribution which completely describes the up-to-date knowledge. It is the necessarily subjective quantification of the prior probability, in particular how to express prior ignorance, which is the cause of debate here. A full comparative discussion of classical, Bayesian and other methods is given by Barnett (1973).

There has been discussion recently about statistical practice in photon counting experiments, most of it from a firmly classical point of view (see, for example, Lampton et al., 1976; Cash, 1979) although the neo-Bayesian approach of Hearn (1969) was used in the presentation of the SAS-2 observations. The technique employed in this paper avoids the hypothetical infinite series of experiments and the subjective prior probability by giving the likelihood "an independent existence" (Edwards, 1972). Likelihood per se is not without its critics though, as Barnett points out.

The basic principle is that if the likelihood of a particular set of data on one hypothesis is larger than the likelihood of the same data on a second hypothesis then the first is more appropriate. However no probability statements can be made about hypothesis. On the other hand if the likelihood ratio $L(H_1)/L(H_2)$ is 10, for example, for two hypotheses H_1 and H_2 then on average H_1 would give the observations 10 times as often as H_2. If a choice is to be made it must be H_1. To proceed in this way, probability models which describe the observations are needed but in the case of COS-B observations of point sources these are fairly straightforward to draw up from calibration measurements. As shown above in Sect. 2, the models reduce to a function of a single unknown parameter, X, the fraction of the observed events which can be attributed to a point source. The data are not binned so maximum use is made of all information available.

The likelihood would also play an important role in both a classical and a Bayesian analysis of the problem. In the former, $X=0$ would be taken as the null hypothesis to be rejected if λ is bigger than typical values obtained through repeated sampling from it. Rather than keeping the data fixed and comparing hypotheses, a hypothesis is fixed and possible observations are studied. As for the Bayesian case, it is a small but important step from the likelihood to the posterior probability distribution but it is one we have not made because of the difficulty of making an objective assessment of the prior probabilities.

References

Apparao, K.M.V., Bignami, G.F., Maraschi, L., Helmken, H., Margon, B., Hjellming, R., Bradt, H.V., Dower, R.G.: 1978, *Nature* **273**, 450
Barnett, V.: 1973, Comparative Statistical Inference, Wiley, New York
Bignami, G.F., Fichtel, C.E., Hartman, R.C., Thompson, D.J.: 1979, *Astrophys. J.* **232**, 649
Bignami, G.F., Bennett, K., Buccheri, R., Caraveo, P.A., Hermsen, W., Kanbach, G., Lichti, G.G., Masnou, J.L., Mayer-Hasselwander, H.A., Paul, J.A., Sacco, B., Scarsi, L., Swanenburg, B.N., Wills, R.D.: 1980, *Astron. Astrophys.* (in press)
Burbidge, G.R., Crowne, A.H., Smith, H.E.: 1977, *Astrophys. J. Suppl.* **33**, 113
Cash, W.: 1979, *Astrophys. J.* **228**, 939
Della Ventura, A., Perotti, F., Villa, G., Di Cocco, G., Butler, R.C., Dean, A.J., Hailes, R.I.: 1979, *Nature* **282**, 484
Edwards, A.W.F.: 1972, Likelihood, C.U.P.
Fichtel, C.E., Simpson, G.A., Thompson, D.J.: 1978, *Astrophys. J.* **222**, 833
Gregory, P.C., Taylor, A.R.: 1978, *Nature* **272**, 704
Gregory, P.C., Taylor, A.R., Crampton, D., Hutchings, J.B., Hjellming, R.M., Hogg, D., Hvatum, H., Gottlieb, E.W., Feldman, P.A., Kwork, S.: 1979, *Astron. J.* **84**, 1030
Hearn, D.: 1969, *Nucl. Instr. Meth.* **70**, 200
Hermsen, W.: 1980, Ph. D. Thesis, University of Leiden, The Netherlands
Kraan-Korteweg, R.C., Tammann, G.A.: 1979, ESO Preprint nº 42
Lampton, M., Margon, B., Bowyer, S.: 1976, *Astrophys. J.* **208**, 177
Marshall, F.E., Mushotzky, R.F., Boldt, E.A., Holt, S.S., Rothschild, R.E., Serlemitsos, P.J.: 1978, *Nature* **275**, 624
Mayer-Hasselwander, H.A., Bennett, K., Bignami, G.F., Buccheri, R., D'Amico, N., Hermsen, W., Kanbach, G., Lebrun, F., Lichti, G.G., Masnou, J.L., Paul, J.A., Pinkau, K., Scarsi, L., Swanenburg, B.N., Wills, R.D.: 1980, Ninth Texas Symposium on Relativistic Astrophysics, in "Annals of the New York Academy of Sciences" **336**, 211
Perotti, F., Della Ventura, A., Villa, G., Di Cocco, G., Butler, R.C., Dean, A.J., Hayles, R.I.: 1980, *Astrophys. J.* **239**, L49
Stein, W.A., O'Dell, S.L., Strittmatter, P.A.: 1976, *Ann. Rev. Astron. Astrophys.* **173**
Swanenburg, B.N., Bennett, K., Bignami, G.F., Caraveo, P., Hermsen, W., Kanbach, G., Masnou, J.L., Mayer-Hasselwander, H.A., Paul, J.A., Sacco, B., Scarsi, L., Wills, R.D.: 1978, *Nature* **275**, 298
Weedman, D.W.: 1977, *Ann. Rev. Astron. Astrophys.* **69**
Wills, R.D., Bennett, K., Bignami, G.F., Buccheri, R., Caraveo, P., D'Amico, N., Hermsen, W., Kanbach, G., Lichti, G.G., Masnou, J.L., Mayer-Hasselwander, H.A., Paul, J.A., Sacco, B., Swanenburg, B.N.: 1980, in *Non-Solar γ-rays* (COSPAR), eds. R. Cowsick and R.D. Wills, Pergamon Press, Oxford, New York, p. 43